

Search for Superconductivity in Ultra-dense Deuterium $D(-1)$ at Room Temperature: Depletion of $D(-1)$ at Field Strength >0.05 T

Patrik U. Andersson · Leif Holmlid · Stephan Fuelling

Received: 10 November 2011 / Accepted: 22 November 2011 / Published online: 21 December 2011
© Springer Science+Business Media, LLC 2011

Abstract Ultra-dense deuterium $D(-1)$ is expected to be both a superfluid and a superconductor as shown by recent theoretical research. Condensed $D(-1)$ can be deposited on surfaces by a source which produces a stream of clusters. A magnetic field strongly influences the type of material formed. Very little of $D(-1)$ and of the form $D(1)$, which is strongly coupled to $D(-1)$, exists on the magnet surface or within several mm from the magnet surface. Even the formation of $D(-1)$ on the source emitter is strongly influenced by a magnetic field, with a critical field strength in the range 0.03–0.07 T. Higher excitation levels $D(2)$ and $D(3)$ dominate in a magnetic field. The excitation level $D(2)$ is now observed for the first time. The removal of $D(-1)$ and $D(1)$ in strong magnetic fields is proposed to be due to a Meissner effect in long $D(-1)$ clusters by large-orbit electron motion. The lifting of long $D(-1)$ clusters above the magnet surface is slightly larger than expected, possibly due to the coupling to $D(1)$. The previously reported oscillation between $D(-1)$ and $D(1)$ in an electric field is proposed to be due to destruction of $D(-1)$.

Keywords Ultra-dense deuterium · Superconductor · Coulomb explosion · Magnetic field

1 Introduction

The ultra-dense deuterium material $D(-1)$ with an experimentally observed D-D distance of 2.3 pm [1–4] may be both superfluid and superconducting. A deuterium phase at greater than atomic densities has been predicted by Berezhiani et al. [5] to be a quantum liquid showing both superfluid and superconducting properties. The different phases of this type of material have been discussed by Bedaque et al. [6]. The quantum mechanical basis for $D(-1)$ was further discussed by Winterberg [7, 8], suggesting the short-distance bonding of deuterons by exchange forces. The special features of the Coulomb explosion (CE) processes in $D(-1)$ indicated early that this material is superfluid at room temperature [1, 9]. This is based both on the well-defined energy of the neutral particles ejected and on the facile energy flow inside the material prior to the CE. Rapid transport of $D(-1)$ over solid surfaces and in capillaries was observed to take place against gravity [10] proving it to be superfluid. In the present contribution, we study the properties and especially the cluster composition of $D(-1)$ in a magnetic field. We here observe a Meissner effect in agreement with the theoretical predictions that $D(-1)$ is superconductive.

Ultra-dense deuterium $D(-1)$ has been studied in our laboratory with laser-induced mass spectrometry (TOF-MS) and neutral time-of-flight energy measurements in several publications [1–4]. Due to the extremely high density of $D(-1)$, of the order of 10^{29} cm⁻³ (140 kg cm⁻³) it is believed to be very useful as target material for inertial confinement fusion (ICF) using intense pulsed lasers [1, 2, 9]. The first experiments showing laser-induced fusion in $D(-1)$ were recently described [11, 12]. The excitation level of dense $D(1)$ and ultra-dense $D(-1)$ materials is generally indicated as $D(l)$, where l is the angular momentum quantum number for the conduction electrons. The basis for the

P.U. Andersson · L. Holmlid (✉)
Atmospheric Science, Department of Chemistry, University
of Gothenburg, 412 96 Göteborg, Sweden
e-mail: holmlid@chem.gu.se

S. Fuelling
University of Nevada Reno, Department of Physics,
1664 N. Virginia Street, Reno, NV 89557-0220, USA

description of $D(-1)$ is that this material is an inverted form of $D(1)$, where the deuterons and the electrons seem to have exchanged their roles. This is based on the general ideas of dense hydrogen materials by Ashcroft and other authors [13, 14]. Only hydrogen isotope atoms are expected to give an ultra-dense material form, since the inner electrons prevent this inversion for all other atoms.

2 Theory

$D(1)$ and $D(-1)$ are the two lowest excitation levels of deuterium Rydberg Matter (RM) [15, 16]. The conduction band electrons in RM in general are excited and delocalized, but in $D(1)$ and $D(-1)$ the electrons are in their lowest energy state which is more complex than for RM in general due to the special quantum mechanical properties. In RM, the potential for the conduction electrons is neither central due to the similar distances to several ions, nor of the form $1/r$ [17]. This means that the only good quantum numbers are the orbital quantum number l and electron and nuclear spin quantum numbers. To distinguish between the quantum numbers for free atoms and the condensed phase, the excitation level n_B (B for Bohr model) is introduced, numerically equal to the orbital electron angular momentum l . RM at excitation levels $n_B = 3 - 8$ is normally observed in the form of planar six-fold symmetric clusters with magic numbers $N = 7, 19, 37, 61,$ and 91 [17, 18]. Independent proof of Rydberg (RM) species formation at alkali promoted catalyst surfaces used as RM emitters exists [19–21]. EPR studies and DFT cluster model calculations of such K doped catalyst materials show an expanded state of the K atom resembling a Rydberg state in the solid phase [22]. Recent results from groups studying cold Rydberg gases show many-particle effects [23–25] which may be related to the RM bonding.

When a laser pulse passes through a material like $D(1)$ or $D(-1)$, the photons may excite (displace) a few electrons so that two ions become exposed to each other. CE makes the ions move apart rapidly, in <1 fs for $D(-1)$. When the CE takes place, the ions fly apart with almost all their repulsion energy as kinetic energy release (KER) in the ionic fragments. It is possible to determine the initial repulsion energy between the ions by measuring the kinetic energy of the fragments at a large distance from the actual explosion event. Then the distance between the ions before the CE, i.e., the bond length is found directly from the Coulomb formula as

$$r = \frac{1}{4\pi\epsilon_0} \frac{e^2}{E_{\text{kin}}} \quad (1)$$

where ϵ_0 is the vacuum permittivity, e the unit charge and E_{kin} the sum kinetic energy for the fragments (KER) from the CE. The fraction of the KER that is observed on each

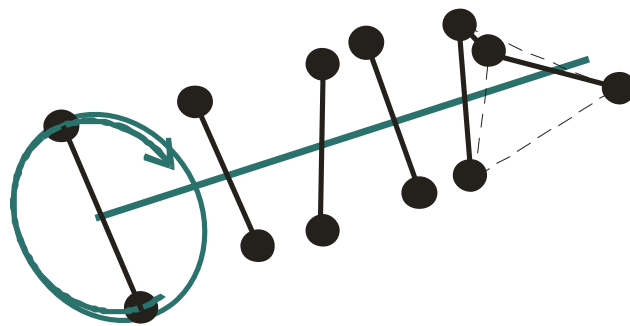


Fig. 1 Shape of the chain or “bead” clusters forming the superconductive phase $D(-1)$. In the superconductive state, the electrons orbit around the cluster

fragment depends of course on the mass ratio of the fragments. The kinetic energy is determined most easily by measuring the time-of-flight (TOF) of the particles and converting this quantity to kinetic energy. This requires that the mass of the particle is known or can be inferred, which is simplified when working with only deuterium.

Dense deuterium $D(1)$ is in most respects similar to $H(1)$ [26]. This means that the interatomic bonding distance d_1 derived from the observed KER of 9.4 eV is close to $2.9 \times 52.9 \text{ pm} \approx 153 \text{ pm}$ [26]. The $H(1)$ clusters can be both planar, as for higher RM levels, and also three-dimensional like tetrahedrons and octahedrons. Recently, the bond distances and forms of the $H(1)$ clusters was studied with a phase-delay method, giving high precision results [27]. The energy level of $D(-1)$ is slightly lower than that of $D(1)$. The interconversion between $D(1)$ and $D(-1)$ is reported to be facile and showing an oscillatory behavior in time [2]. Further details of the conversion are given in Ref. [28]. A theoretical description of $D(-1)$ was recently given by Winterberg. This stresses the similarity to other superfluids and proposes that exchange forces are responsible for the strong bonding of the deuterons in the material [7, 8]. The observed KER of up to 630 eV gives a bond distance of $2.3 \pm 0.1 \text{ pm}$ under normal conditions [1, 2]. At lower temperature, the bond distance was recently found to be $2.14 \pm 0.03 \text{ pm}$ [4]. These values are close to the theoretically expected distance for an inverted $D(-1)$ material of $d_{-1} = (m_e/m_D)^{1/2}d_1$ equal to 2.5 pm [1].

The form of the clusters composing $D(-1)$ can be found from the fragment patterns in the CE experiments. All available information indicates that they are chain clusters or “bead” clusters of the form D_{2N} with N an integer, as shown in Fig. 1. Each bead is formed by a pair d–d which rotates around the common mass center. Such a pair may be formed by exchange forces [7, 8]. Several d–d pairs form the bead clusters. The electrons form a vortex in each bead cluster. Thus, each such cluster can show a Meissner effect. The attraction forces due to the electrons which are likely to exist close to the mass center of the d–d pair probably also

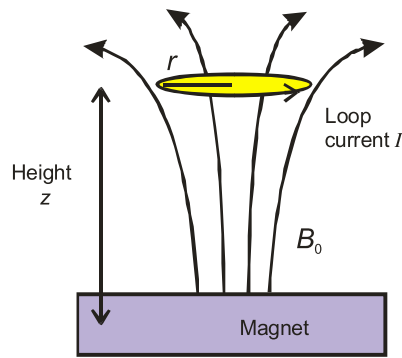


Fig. 2 Balancing of a superconductive cluster in the magnetic field at a distance z above the center of the magnetic dipole. The current loop with current I shown has a radius r

take part in the formation of the pair. In the superconducting state some electrons have orbits with large dimensions, as described by Hirsch [29]. The superconducting state thus corresponds to a state with orbiting electrons, similar to an ordinary RM cluster state. Small clusters D_2 and D_4 [4] will not be able to support any preferential direction of the cluster or a vortex, and they will probably not be able to give a Meissner effect. Thus, such small clusters will not lift in the strong magnetic field at the surface of the magnets used in the experiments described below.

When the magnet in the experiments lies flat horizontally with the magnetic field in the vertical direction, superconductive material on top of the magnet may float in the magnetic field at a distance from the magnet. This situation is shown schematically in Fig. 2. It is assumed that the superconductive current in the large $D(-1)$ clusters forms a circular loop, to simplify the calculation of the magnetic moment in the cluster. This is in agreement with the large electron orbits proposed to exist in type-II superconductors [29]. The weight of the cluster containing N deuterium atoms is balanced by the magnetic force due to the Meissner effect. The force results from the expulsion of magnetic flux over the area of the deuterium cluster. The repulsion can be viewed as the repulsive force between two magnetic dipoles, the magnetic dipole moment of the permanent magnet and the opposing magnetic moment of the deuterium cluster. The magnetic moment of the magnet can be approximated by

$$m_M = B_0 V_M / \mu_0 \tag{2}$$

where B_0 is the magnetic field of the magnet close to its surface, V_M is the total volume of the magnet and μ_0 is the vacuum permeability. The magnetic field at a distance z above the center of the magnet is approximated as

$$B_M(z) = \mu_0 m_M / (2\pi z^3). \tag{3}$$

Equating the magnetic field due to the superconducting loop with that from the magnet at height z gives the required superconductive current as

$$I = B_0 V_M r / (\pi \mu_0 z^3) \tag{4}$$

with r the radius of the superconductive loop in the cluster. The repulsive force between the cluster and the magnet is equal to the gravitational force on the cluster. This gives the balancing height above the center of the magnet

$$z = \left(\frac{3 B_0^2 V_M^2 r^3}{2\pi \mu_0 M g} \right)^{1/7} \tag{5}$$

where g is the acceleration of gravity. The mass of the cluster M is probably not independent of the radius of the current loop r . If the total mass scales with distance r^3 , the distance z will be independent of cluster size. It is then more informative to calculate the radius r of the current loop in a fictitious one-atom cluster with mass m , which is

$$r = \left(\frac{2\pi \mu_0 m g z^7}{3 B_0^2 V_M^2} \right)^{1/3} \tag{6}$$

For a real small permanent magnet, the variation of B with distance is different from that in (3). It is possible to model the magnetic field on the centerline of a cylindrical magnet by

$$B(z) = C \frac{x_{\max}^2}{(x_{\max}^2 + z^2)^{3/2}} \tag{7}$$

where x_{\max} is the approximate radius of the magnet pole face, and $z = z_F + z_0$ is the sum of the distance z_F from the magnet face and of an offset z_0 due to the thickness of the magnet. C is a constant for the special magnet found by a fit to the measured magnetic field strength at a few distances z . The magnet is assumed to be two-dimensional (a good approximation in our case). Similar expressions have been derived also for 3D magnets with similar fits to the magnetic field strength. By inserting the distance z it is then possible to find the magnetic field $B(z)$ and its derivative with respect to this distance $B'(z)$, giving the radius of the current loop for a fictitious one-atom cluster in the field from the real magnet as

$$r = \left(\frac{\mu_0}{2\pi} \frac{m g}{B(z) B'(z)} \right)^{1/3} \tag{8}$$

3 Experimental

The apparatus has been described in several publications, for example, in [26]. The new central source part is described separately [3]. The emitter is as before a cylindrical (extruded) sample of an industrial iron oxide catalyst doped with K (initially at 8 wt%) [30, 31]. It is of the styrene catalyst type Shell S-105 which is an efficient hydrogen abstraction and transfer catalyst. The emitter is mounted in the tight-fitting opening of a metal tube which is connected to the D_2 gas feed. The catalyst can be moved relative to the center of the vacuum chamber, which has a base pressure $< 1 \times 10^{-6}$ mbar. The source metal tube is heated by an

Fig. 3 Two different experiments. The angle between the laser and the particle beams is 45° . The plate can be placed in any position below the source. The horizontal plate has a diameter of 30 mm. In (a) one experiment with the magnet on the sloping support is shown, with results in Fig. 6, middle trace. In (b) the source is in contact with the magnet which lies flat on the horizontal plate, with results in Fig. 8

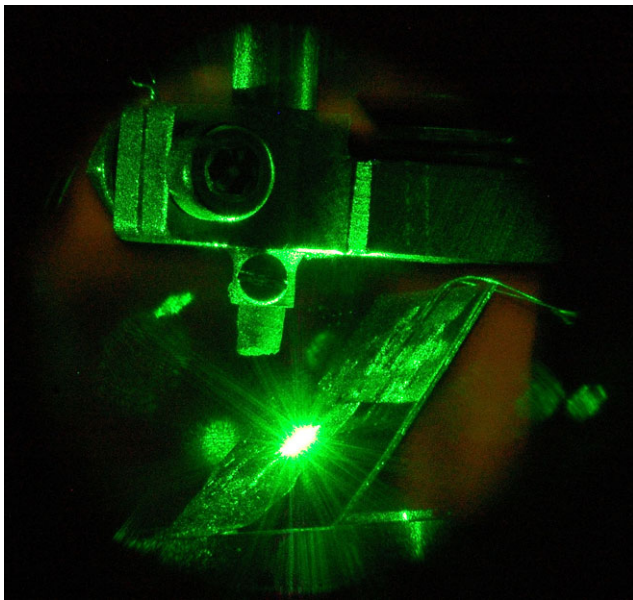
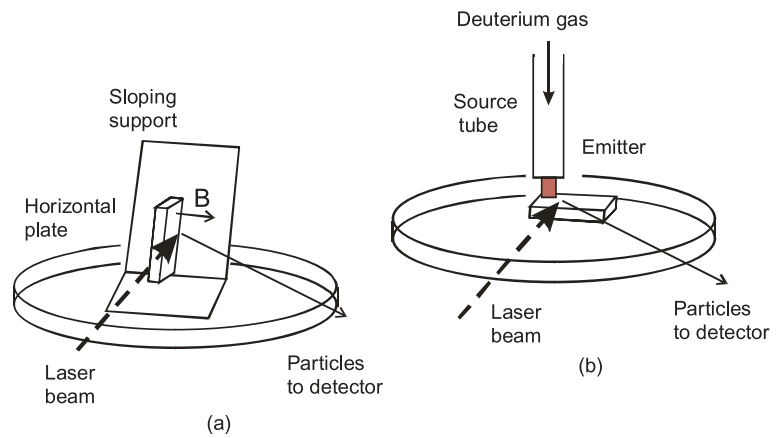


Fig. 4 Experiment with magnet and a Ta foil, with the magnet behind the foil to the left. The laser hits the foil on the part of the foil with no magnet below. The shadow of the Ta foil is observed on the sloping support to the right. The source is seen in the upper half of the figure. The viewing angle is at 90° relative to the laser beam

AC current through its wall up to 400 K. Deuterium gas ($>99.8\%$ D_2) is admitted through the source at a pressure up to 1×10^{-5} mbar in the chamber. The $D(-1)$ falls down as clusters to a stainless steel plate with 3 cm diameter below the source. The plate has a rim (flange) to prevent the fluid from dripping off too fast, as shown in Fig. 3. On this plate different items are placed, like a sloping metal surface at 45° angle towards the horizontal as in (a). A NdFeB magnet (SSG N33SH) with dimensions $3 \times 4 \times 8$ mm³ is used to give a magnetic field strength up to 0.17 T at 1.0 mm distance, with the largest faces being the pole faces (the manufacturer states that the remanent field strength B_r is > 1.1 T). The magnet has been used in many orientations,

with two examples shown in Fig. 3. In this figure, the direction to the detector at 45° relative to the incoming laser beam is also indicated. An 0.1 mm thick Ta foil is used in some experiments, with an example in Fig. 4, to cover the magnet and an area outside the magnet. In this way direct comparisons with and without a magnetic field are possible, avoiding other material and geometric effects. A Nd:YAG laser with an energy of < 100 mJ per each 5 ns long pulse at 10 Hz is used at 532 nm. The laser beam is focused at the center of the UHV chamber with an $f = 400$ mm spherical lens. The intensity in the beam waist of (nominally) 70 μ m diameter is relatively low, $\leq 10^{12}$ W cm⁻² as calculated for a Gaussian beam. The detector is a dynode–scintillator–photomultiplier setup [26]. The detector is here located at an angle of 45° from the incoming laser beam and measures the time-of-flight (TOF) spectra of fast neutral or ionized particles from the CE process since no accelerating voltage is employed. The fast particles impact on a stainless steel (catcher) foil in the detector, and fast ions ejected from there are drawn towards a Cu–Be dynode held at -7.0 kV inside the detector. The total effective flight distance for the ions from the laser focus to the catcher foil is 101 mm by direct measurement and internal calibration [1, 28]. The photomultiplier (PMT) is Electron Tubes 9128B with single electron rise time of 2.5 ns and transit time of 30 ns. Blue glass filters in front of the PMT decrease the observed laser signal. A fast preamplifier (Ortec VT120A, gain 200, bandwidth 10–350 MHz) is used. The signal from the PMT is studied and collected on a fast digital oscilloscope (Tektronix TDS 3032, 300 MHz) which displays the signal correctly even when the signal is large, or in a multi-channel scaler (EG&G Ortec TurboMCS) with dwell time 5 ns per channel. Each MCS spectrum consists of a sum of the signals from 250 laser shots. The digital average mode is sometimes used in the oscilloscope.

Fig. 5 Magnet lying flat on the horizontal support in the upper oscilloscope trace, with horizontal laser beam passing the magnet to the distant beam dump. In the lower trace, part of the beam hits the small front edge of the magnet. Laser power 70 mJ. Single-shot spectra

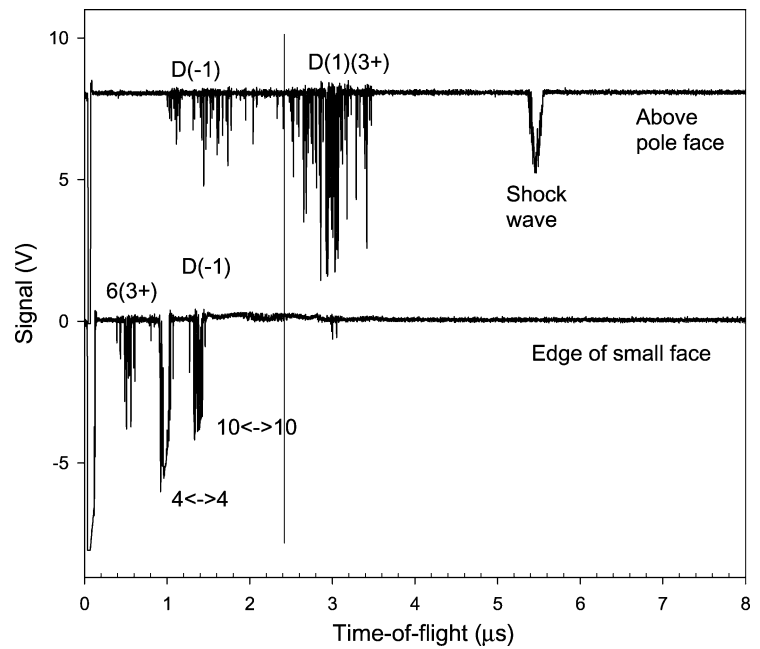


Table 1 Symmetric fragmentation of D(−1) clusters with flight times *t* in the present experiments

| Total charge | Total cluster mass | Name | <i>t</i> ₁ , <i>t</i> ₂ (ns) | <i>t</i> ₃ , <i>t</i> ₄ (ns) |
|--------------|--------------------|---------|--|--|
| 4 | 8 | 8 (4+) | ≈336 | ≈336 |
| 3 | 6 | 6 (3+) | ≈412 | ≈412 |
| 2 | 40 | 20 ↔ 20 | 1841 | |
| | 36 | 18 ↔ 18 | 1746 | |
| | 32 | 16 ↔ 16 | 1646 | |
| | 28 | 14 ↔ 14 | 1540 | |
| | 24 | 12 ↔ 12 | 1426 | |
| | 20 | 10 ↔ 10 | 1302 | |
| | 16 | 8 ↔ 8 | 1164 | |
| | 12 | 6 ↔ 6 | 1008 | |
| | 8 | 4 ↔ 4 | 823 | |
| | 4 | 2 ↔ 2 | 582 | |

4 Results

4.1 Probing on the Magnet

Various orientations have been used for the magnet to study the influence of the magnetic field. Just a few examples are shown here. With the magnet flat in the horizontal plane, the laser beam can pass just above the pole face. In the top trace in Fig. 5 it is seen that the intensity due to D(−1) and especially the signal corresponding to small clusters is strongly decreased in this case. The interpretation given is based on the calculated TOFs in Tables 1 and 2. This effect could

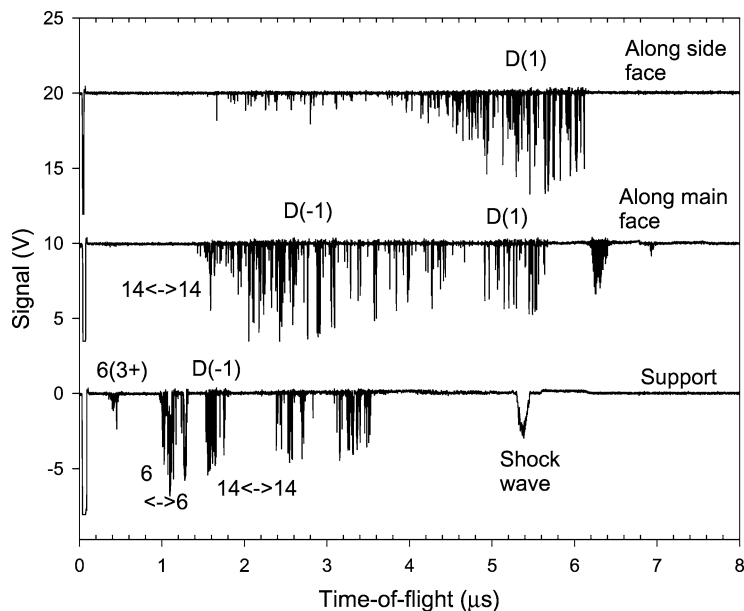
Table 2 The shortest possible TOF for D⁺ (repelled from infinite mass) from asymmetric CE processes with 2 and 3 charges in the D(RM) cluster

| Excitation level | 2+ | 3+ |
|------------------|---------|--------|
| D(−1) | 411 ns | 291 ns |
| D(1) | 3.4 μs | 2.4 μs |
| D(2) | 6.7 μs | – |
| D(3) | 10.1 μs | – |
| D(4) | 13.5 μs | – |

partly be due to a lower density of the deuterium materials above the magnet. However, a clear shock-wave is observed to be formed by the CE process above the magnet, which indicates a high density. When the laser beam is lowered slightly to hit the edge of the magnet, fast particles from D(−1) are observed, in the bottom trace in Fig. 5. Thus, small D(−1) clusters are observed with a direct laser hit on the magnet surface in Fig. 5 while large clusters of D(−1) and also D(1) are observed above the magnet surface. This indicates a lifting of large D(−1) clusters from the surface by a Meissner effect.

When the magnet is mounted as in Fig. 3(a), the situation is different for the probing laser, since the beam is stopped by the stainless steel support against which the magnet is leaning. The two traces at the top in Fig. 6 show the signal with the laser beam along but not directly hitting the magnet surfaces. The results are similar to those in Fig. 5 with small D(−1) clusters lacking outside the magnet surface. However, a considerable density of larger clusters of D(−1) is obtained, as well as of D(1). In the bottom trace in Fig. 6, the spectrum from the support shows more small D(−1) clusters. The conclusion is the same as from Fig. 5,

Fig. 6 Magnet supported by sloping stainless steel plate. See Fig. 3(a) for orientation in one case, with laser beam along main face of the magnet. Laser beam at 45 mJ is along one face of the magnet and hits the support close to the magnet. Single-shot TOF spectra



namely that large $D(-1)$ clusters lift from the magnet surfaces, probably by a Meissner effect.

Thus, the changes in cluster distributions depend on the magnetic field. However, the edges of the magnet and the different materials in the surfaces (support of stainless steel, Ni plated magnet) may still influence the signals observed. That $D(-1)$ is superfluid may also give a rapid flow from the surrounding surfaces to the point of probing, which introduces some uncertainty since the signals observed may either be intrinsic or partly due to transport effects. We now go on to prove that such effects do not influence the results.

4.2 Probing on a Foil Above the Magnet

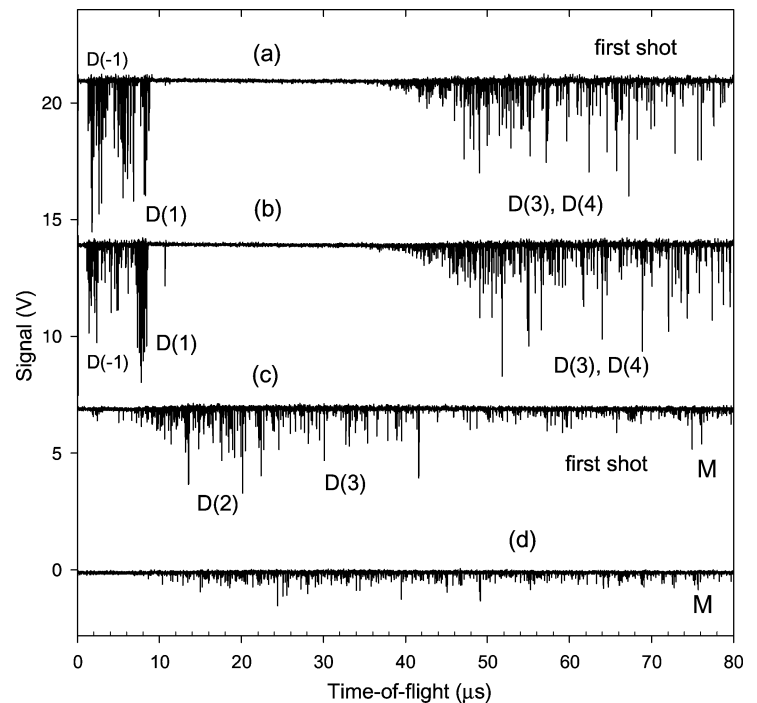
Further experiments have used the setup in Fig. 4. The exposed surface is a Ta foil with 0.1 mm thickness on top of (covering) the magnet and the space to the right of the magnet. Thus, in Fig. 4 the laser to the right on the Ta foil probes a surface with no magnet below. There is a visible difference between the laser impact to the left (with magnetic field) and to the right as in Fig. 4 (no magnetic field). The plasma with no magnetic field is much stronger and appears hotter (whiter) than in the magnetic field. The diameter of the plasma is 2 mm while the mark of the laser beam on the Ta foil has a diameter of 0.2 mm at most. The two positions with and without a magnetic field at 4 mm separation are easily and reproducibly probed by adjusting a mirror at 600 mm distance. The signal ions leaving the point of laser impact move almost along the magnetic field lines, and are thus not deflected by the magnetic field. Due to their large initial kinetic energy from the CE process, the ions would be only weakly influenced even if they moved perpendicular to the magnetic field. The angular distributions of the ejected

ions are broad and a small deflection of the ions will not influence the signal seen by the detector.

Results are shown in Fig. 7 from two different experiments, with TOF up to 80 μs . Spectra (a) and (b) are almost identical, with spectrum (a) being first-shot and spectrum (b) taken with the laser running at 2 Hz at steady-state on the surface position with no magnetic field (to the right). Since the spectra are identical, the material with no magnetic field is superfluid and mainly in the form $D(-1)$ and $D(1)$ and high excitation levels like $D(4)$. On the other hand, spectra (c) and (d) show the signal from the position with magnetic field (to the left in Fig. 4). In this case, the first-shot spectrum differs strongly from the steady-state spectrum, showing that the material in the magnetic field is not superfluid. The material there is mainly in form of $D(2)$ and $D(3)$, while $D(-1)$ and $D(1)$ are missing. A strong difference between the magnet position and the empty position is thus observed, with $D(-1)$ removed from the magnetic field position probably by a Meissner effect.

A direct appreciation of this experiment may require some further description of its background. On the emitter, $D(\text{RM})$ will be formed initially in excitation levels $D(3)$ and $D(4)$ by interaction with the K promoter atoms in analogy with $H(\text{RM})$, as shown in previous studies [1, 32]. The material will easily fall down to lower excitation levels like $D(1)$ and $D(-1)$, as observed on non-magnetic surfaces and in Figs. 5 and 6. On the magnet, the excitation level $D(2)$ is observed for the first time, together with small clusters $D(3)$, apparently since $D(-1)$ and $D(1)$ cannot exist there. The cluster forms of $D(2)$ have not been observed previously, apparently due to its normally rapid deexcitation down to $D(1)$ and to the strongly coupled $D(-1)$ excitation level. It is concluded that the superconductive phase $D(-1)$ does not

Fig. 7 Single-shot oscilloscope TOF spectra at long times, showing the origin of magnetic effect on the cluster distributions. Figure 4 shows the experimental situation. Laser beam at 45 mJ. *M* means that the laser is to the left, hitting the Ta foil covering the magnet in spectra (c) and (d). The two top spectra (a) and (b) are from the position shown in Fig. 4, with no magnet below the sampled part of the foil. “First shot” means the first laser shot after being turned off for approximately one minute, while the other spectra are single-shot measured in steady-state with the laser running at 2 Hz



exist on the sloping surface above the magnet probably since its formation via D(2) and D(1) is impeded by the magnetic field.

4.3 Probing on the Emitter

As a further direct test of the influence of the magnetic field, the emitter in the source is moved to almost touch the magnet in Fig. 8. This means that a strong magnetic field exists at the lower part of the emitter. The normal situation with small and large D(−1) clusters at the emitter then changes and only large D(−1) clusters are observed. The situation is, however, less extreme than in Fig. 7. Averaged spectra are shown in Fig. 8, using both the MCS and the oscilloscope, which proves that signal size effects are not important. (There is a short period between taking the two sets of spectra, meaning that they are not identical but only similar). For comparison, the simultaneous TOF spectrum from probing on the outside of the flange in Fig. 3(b) is shown in both cases in Fig. 8. The signal from the outside of the flange is of the “normal” form with small D(−1) clusters. The strength of this signal shows that D(−1) is superfluid, giving a film easily moving to the outside of the container. It is also concluded directly that even if the material from the emitter is influenced by the magnetic field, it converts to the normally observed D(−1) state when it has moved 1–2 cm away from the magnetic field, to a field strength of the order of 0.05 T or lower at the plate flange. This indicates that superconductive D(−1) which has the form of long chain clusters is not stable in a magnetic field stronger than 0.05 T. This is as ex-

pected for a superconductor [33]. Future studies are likely to give more details on the processes involved.

Another similar experiment in Fig. 9 is quite informative. The emitter is located slightly above the magnet. The laser probes at the emitter at two different positions above the magnet, as shown in the figure. Two averaged spectra are shown, giving direct evidence for a critical magnetic field [33] close to 0.05 T (field strengths at distances from the pole face are manufacturer’s data). A clear transition is observed from the case with no formation of D(−1) at 3 mm distance from the magnet, to the case with small clusters at lower magnetic field strength at larger distance. These results are from the material on the catalytic emitter where both D(1) and D(−1) are formed from deuterium gas, thus this experiment is not related to free clusters above the magnet surface. The observed results are expected for a superconductor [33]. Tests without a magnet were made after this experiment to ascertain that this effect was not due to a variation along the emitter material for some unknown reason. Thus, the magnetic field removes D(−1) and partly also D(1). The critical field is close to 0.05 T.

5 Discussion

The D(−1) phase consists of bead or chain clusters as described in the theoretical section. In the present experiments at low laser intensity mainly symmetric CE processes (thus central cleavage of the bead or chain clusters) are observed, but with high laser intensity asymmetric processes for large

Fig. 8 The effect of a magnetic field on the material produced by the emitter. Averaged TOF spectra with MCS (*top*) and oscilloscope (*bottom*). Laser pulse at 45 mJ. The spectra indicated “plate flange” are from the outside of the flange (rim) of the horizontal plate, shown in Fig. 3. They show the behavior for the emitter without magnetic field, with small clusters $D(-1)$ giving fast particles with kinetic energy above 630 eV. In the magnetic field, only large $D(-1)$ clusters exist on the emitter

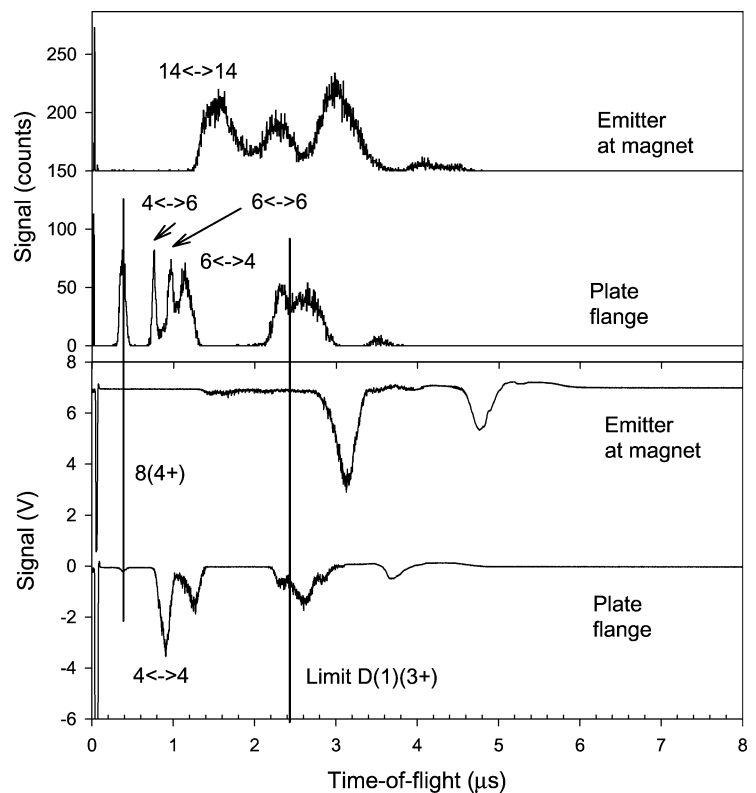
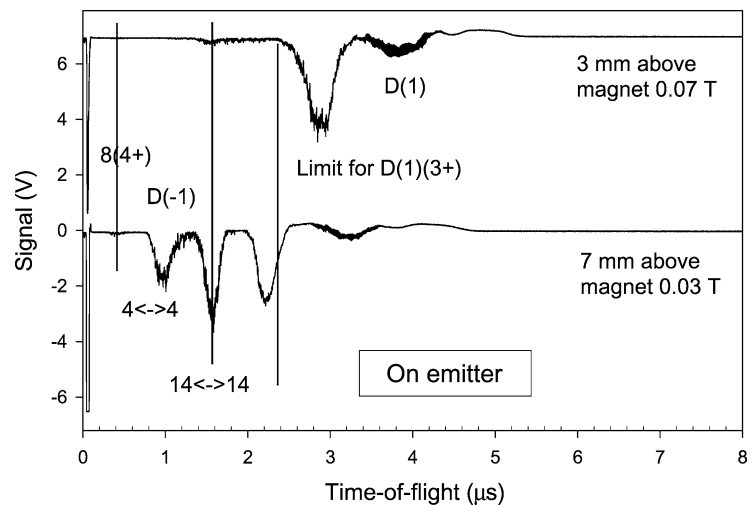


Fig. 9 TOF spectra from the emitter surface at two different distances above the magnet, with stationary source. Laser pulse energy 45 mJ. The *top spectrum* is from the lowest part of the emitter, and the *bottom spectrum* is from the top part of the emitter. The critical field preventing $D(-1)$ from existing on the emitter is in the range 0.03–0.07 T



clusters may dominate. (The asymmetric processes mainly mean ejection of D^+ and D_2^+ from large clusters, presumably from the ends of chain clusters). Small clusters are observed especially as D_3 and D_4 clusters as seen in Table 1 and in the figures. The long chains probably coincide with vortices in the material. Fragmentations like $10 \leftrightarrow 10$ and $14 \leftrightarrow 14$ are assigned in the figures. The first of these could be due to splitting of a D_{10} cluster formed by five such D_2 pairs, giving the CE between the two central D atoms, cleaving a bond of 2.3 pm length. The $14 \leftrightarrow 14$ fragmentation could be similar, cleaving the central D_2 pair of seven

pairs. The cluster chains may work as antennas, channeling the energy to one of the weakest spots in the cluster. In Figs. 6 and 8, also the CE process $6 \leftrightarrow 6$ may be observed. This process can be explained in the same way as the heavier cases, but instead with three D_2 pairs initially. This description is modeled to agree with the concept of d-d pair formation [7, 8, 10] and with the expected rotation of such pairs around the vortices in the $D(-1)$ superfluid.

In [2], we reported on the rapid oscillation between $D(1)$ and $D(-1)$. Such oscillations are only observed with an applied electric field, which is used in the experiment in [2]

to accelerate ions for a TOF-MS study. The logical conclusion from this observation is that one of the two phases is highly conductive and that, after some time, it is destroyed by the current or the accelerated ions. With $D(-1)$ a superconductor, such a simple explanation is indeed possible. This implies that the superconductive $D(-1)$ at the emitter is broken down above a critical current density to a non-superconductive state consisting of small clusters. After the current is removed, the material has to be reconstructed to $D(-1)$, which takes some time, as observed in the experiments [2]. This may give the observed delay and oscillation, and not only a small constant amount of $D(-1)$ in a steady-state as may be expected for most tentative explanations.

An expression for the height above the magnet where the Meissner effect stabilizes the clusters was derived in (5). Such a stabilization is not possible when the magnet is not in the horizontal position, as in the cases in Figs. 3(a) and 4. This means that in these cases the clusters will slide down due to gravity and only a thin cloud of clusters (formed at the surface and lifting due to the magnetic field) should exist above the magnet surface. However, in the experiment in Fig. 5, a collection of clusters above the horizontal magnet is expected and $D(-1)$ clusters are also observed there. The laser beam samples at different values of B close to the edges of the magnet (which is not simulated), but the central magnetic field strength is used here. The values found from (6) and (8) are not identical. In both cases it is apparent that only a superconductive cluster can lift in this relatively weak magnetic field. In the limit of being at the magnet surface ($z = 1.5$ mm), the radius of the current loop r becomes 1.3 pm in the theoretical dipole field used for (6). The field strength used at the surface of the magnet of 0.27 T was found from the fitting to the expression in (7). The real magnetic field with (8) gives a loop radius of 6.3 pm. Both values are in the pm range, which is reassuring since the clusters have dimensions in the pm range, but the larger value using the real field should be more reliable. This may indicate that the clusters have a larger magnetic moment than the sum of the fictitious one-atom clusters forming the larger clusters, or that the macroscopic description that we use is insufficient to describe the behavior of the clusters in the magnetic field.

It is apparent from the experiments that small clusters like D_3 and D_4 are not superconductive and that they will not float in the field. If the $D(-1)$ clusters were not superconductive but diamagnetic, they would not be able to float in the magnetic field but would sink to the surface of the magnet. Thus, large $D(-1)$ clusters are concluded to be superconductive from their magnetic lifting behavior (a Meissner effect). From the results in Fig. 5, it might appear that also $D(1)$ clusters are superconductive, since they float as the $D(-1)$ clusters do. As described above, $D(1)$ clusters may be similar to $D(-1)$ clusters in their structure, having

the form of chains of small clusters and D_2 pairs. This form might be superconductive. However, superconductive current loops like those discussed for $D(-1)$ would lift $D(1)$ clusters far out from the magnet. Due to the much larger dimensions of the $D(1)$ clusters, it is clearly sufficient if they were diamagnetic to float in the magnetic field. The intimate relation between $D(1)$ and $D(-1)$ involving rapid transformations between these two forms of the material may mean that the average size of the clusters is larger than what the bond distance of 2.3 pm for the $D(-1)$ would indicate. Thus, the lifting observed may be due to the transformation or coupling of $D(-1)$ to the form $D(1)$. It is also possible that the electron orbits in the superconducting cluster are larger than the size of the cluster, forming Rydberg-like orbits [29].

6 Conclusions

Ultra-dense deuterium $D(-1)$ is predicted to be a superconductor type-II at room temperature. Here we show that a magnetic field stronger than approximately 0.05 T prevents the formation of, and even removes the $D(-1)$ material from the magnetic field. The observed lifting of the clusters from the magnet surface agrees with theory for the Meissner effect. Each chain or bead cluster of $D(-1)$ probably contains a central vortex, and it will have electrons with large orbits in the superconductive state. The experiments show strong magnetic effects and in the Coulomb explosion spectra, $D(-1)$ is missing completely in a magnetic field stronger than 0.05 T. The removal of $D(-1)$ and $D(1)$ is gradual with increasing field strength, with critical field strength in the range 0.03–0.07 T. At high field strength, only higher excitation levels $D(2)$ and $D(3)$ exist. Of these levels, $D(2)$ is observed for the first time. Dense deuterium $D(1)$ is in rapid equilibrium with $D(-1)$. The previously reported rapid oscillation between $D(1)$ and $D(-1)$ is proposed to be due to the destruction of superconduction in $D(-1)$ by current transport. The coupling between $D(1)$ and $D(-1)$ may be one reason for the strong Meissner effect observed for large $D(-1)$ clusters.

References

1. Badiei, S., Andersson, P.U., Holmlid, L.: Phys. Scr. **81**, 045601 (2010)
2. Badiei, S., Andersson, P.U., Holmlid, L.: Appl. Phys. Lett. **96**, 124103 (2010)
3. Andersson, P.U., Lönn, B., Holmlid, L.: Rev. Sci. Instrum. **82**, 013503 (2011)
4. Holmlid, L.: Int. J. Mass Spectrom. **304**, 51 (2011)
5. Bereziani, L., Gabadadze, G., Pirtskhalava, D.: J. High Energy Phys. **4**, 94 (2011)
6. Bedaque, P.F., Buchoff, M.I., Cherman, A.: J. High Energy Phys. **4**, 122 (2010)
7. Winterberg, F.: J. Fusion Energy **29**, 317 (2010)

8. Winterberg, F.: *Phys. Lett. A* **374**, 2766 (2010)
9. Andersson, P.U., Holmlid, L.: *Phys. Lett. A* **373**, 3067 (2009)
10. Andersson, P.U., Holmlid, L.: *Phys. Lett. A* **375**, 1344 (2011)
11. Badiei, S., Andersson, P.U., Holmlid, L.: *Laser Part. Beams* **28**, 313 (2010)
12. Andersson, P.U., Holmlid, L.: *J. Fusion Energy* (2011, in print) doi:[10.1007/s10894-011-9468-2](https://doi.org/10.1007/s10894-011-9468-2)
13. Ashcroft, N.W.: *J. Low Temp. Phys.* **139**, 711 (2005)
14. Militzer, B., Graham, R.L.: *J. Phys. Chem. Solids* **67**, 2136 (2006)
15. Manykin, E.A., Ojovan, M.I., Poluektov, P.P.: *Proc. SPIE* **6181**, 618105-1-9 (2006)
16. Manykin, É.A., Ozhovan, M.I., Poluéktov, P.P.: *Sov. Phys. JETP* **75**, 440 (1992)
17. Holmlid, L.: *Chem. Phys.* **237**, 11 (1998)
18. Holmlid, L.: *J. Mol. Struct.* **885**, 122 (2008)
19. Kotarba, A., Dmytrzyk, J., Narkiewicz, U., Baranski, A.: *React. Kinet. Catal. Lett.* **74**, 143 (2001)
20. Kotarba, A., Baranski, A., Hodorowicz, S., Sokolowski, J., Szytula, A., Holmlid, L.: *Catal. Lett.* **67**, 129 (2000)
21. Kotarba, A., Adamski, G., Sojka, Z., Witkowski, S., Djega-Mariadassou, G.: *Stud. Surf. Sci. Catal.* **130A**, 485 (2000)
22. Chiesa, M., Giamello, E., Di Valentin, C., Pacchioni, G., Sojka, Z., Van Doorslaer, S.: *J. Am. Chem. Soc.* **127**, 16935 (2005)
23. Mourachko, I., Li, W., Gallagher, T.F.: *Phys. Rev. A* **70**, 031401 (2004)
24. Anderson, W.R., Robinson, M.P., Martin, J.D.D., Gallagher, T.F.: *Phys. Rev. A* **65**, 063404 (2002)
25. Choi, J.-H., Knuffmann, B., Cubel Liebisch, T., Reinhard, A., Raithel, G.: *Adv. At. Mol. Opt. Phys.* **54**, 132 (2006)
26. Badiei, S., Holmlid, L.: *J. Phys. B. At. Mol. Opt. Phys.* **39**, 4191 (2006)
27. Holmlid, L.: *J. Nanopart. Res.* **13**, 5535 (2011)
28. Holmlid, L.: *J. Clust. Sci.* (2011, in print) doi:[10.1007/s10876-011-0387-1](https://doi.org/10.1007/s10876-011-0387-1)
29. Hirsch, J.E.: *Physica C* **470**, 635 (2010)
30. Meima, G.R., Menon, P.G.: *Appl. Catal. A, Gen.* **212**, 239 (2001)
31. Muhler, M., Schlögl, R., Ertl, G.: *J. Catal.* **138**, 413 (1992)
32. Kotarba, A., Holmlid, L.: *Phys. Chem. Chem. Phys.* **11**, 4351 (2009)
33. Guénault, T.: *Basic Superfluids*. Taylor & Francis, London (2003)